Catalytic Transformation of Toluene over High Acidity Y-Zeolite Based Catalyst

S. Al-Khattaf*

Chemical Engineering Department, King Fahd University of Petroleum & Minerals
Dhahran 31261, Saudi Arabia

Abstract

Catalytic transformation of toluene has been investigated over Y-zeolite based catalysts in a novel riser simulator at different operating conditions. A number of experiments were carried out in the temperature range of 400-500^{o}C to understand the transformation of toluene over high acidity Y-based zeolite catalyst (H-Y). It has been observed that toluene can transform either through disproportionation producing benzene and xylene isomers or through dealkylation producing gases and benzene. The rate of both reactions essentially depends on reaction temperature. Dealkylation reaction was found to be favored by high temperature. The benzene/xylene ratio was found to increase with temperature due to the high xylenes dealkylation rate. Toluene transformation was found to be controlled by both Y-zeolite acidity and reaction temperature. While high acidity and high reaction temperature favor toluene dealkylation, medium acidity and low reaction temperature favor toluene disproportionation. Pseudo-homogenous first order kinetic was used to model toluene conversion. Two different deactivation functions were included in this model and the kinetic constants were calculated based on these two different functions.

Feb 2006

Keywords: Toluene; Xylenes ; USY; Toluene Disproportionation; Toluene dealkylation.

*Corresponding author. Tel.: +966-3-860-1429; Fax: +966-3- 860-4234
e-mail address: skhattaf@kfupm.edu.sa

1. Introduction

The demand for xylenes as raw material for polyester fibers and films continues to grow and drive the search to increase xylene production processes. One common way for xylene production is conversion of the lower value toluene (C_7) into xylenes. Huge research has been devoted for this purpose. It is well known that toluene undergoes several simultaneous chemical reactions which include; disproportionation, transalkylation, dealkylation, and coke formation.

Toluene transformation is well documented in the literature [1-6]. This transformation can take place through two major different techniques. The first is toluene hydrodealkylation where toluene is converted to benzene in the presence of hydrogen. The other technique is disproportionation where two toluene molecules react together to form benzene and xylene. Mobil disproportionation process (TDP-3^{SM}) is among the most famous commercial processes for toluene disproportionation [7]. Most of the reported studies on toluene disproportionation have been conducted at relatively high pressure and in the presence of hydrogen using a fixed bed reactor. ZSM-5 zeolites can be used in toluene disproportionation to enhance *para*-selectivity to higher than 90% [4-6].

Pacheco Filho et al [8] carried out toluene disproportionation over a commercial mordenite catalyst in the presence of hydrogen. The toluene conversion was found to increase steadily as the temperature was raised but decreased with increase in space velocity. The catalyst was impregnated with 8.5 wt% of phosphorus to enhance p-xylene selectivity. Peng et al [9] studied toluene transformation over dealuminated MCM-22 zeolites. The activity of MCM-22 was found comparable to that of mordenite and much higher than that of ZSM-5. The fraction of p-xylene in xylene isomers (para-selectivity) formed on MCM-22 was higher than its equilibrium value, and increased further by the dealumination due to the elimination of the framework Al atoms predominantly on the external surface and inside the 10-MR channels. Kaeding et al [5] were able to produce benzene and xylenes rich in the para isomer (70–90%) over ZSM-5 zeolites which were modified with phosphorus, boron, or magnesium compounds. The increment of p-xylene selectivity is due to the reduction of the dimensions of pore openings and channels sufficiently to favor formation and outward diffusion of p-xylene, the isomer with the smallest minimum dimension. Kunieda et al [10] studied more than 20 kinds of the synthesized ZSM-5 to investigate the source of selectivity of p-xylene formation. They suggested that p-xylene selectivity could be correlated with not only the diffusion rate but

also the external solid acidity. Zheng et al [11] modified HZSM-5 with antimony oxide to enhance diffusional constraints and to remove the unselective Brønsted acid sites which led to enhance p-xylene selectivity.

Auer and Hofmann [12] studied the pore structure and the acidic properties of pillared clays based on montmorillonite and hectorite intercalated with aluminium-, zirconium- and chromium-hydroxy oligomers. They found that the catalytic activity of the optimal Cr-pillared clay is between the activities of H-ZSM-5 and an H-Y-zeolite. Gang Yang et al [13] investigated toluene reactions on hybrid catalysts composed of physically mixed NiS/SiO_2 and USY zeolite. It was suggested that hydrogen species supplied by hydrogen spillover at NiS sites and inter-particle migration promote toluene disproportionation. Davidova et al [14] pointed out that nickel-zeolite catalysts in the reduction form are active for toluene dealkylation and under certain conditions for the disproportionation reaction.

Two typical transalkylation side reactions exist in toluene disproportionation; the first one is the reaction between toluene and the produced xylene and the second one is the reaction between two produced xylenes. Xylene dealkylation is a very important secondary reaction especially with high acidity catalyst [15]. The first two secondary reactions form tri-methyl-benzene (TMB) and xylene dealkylation reaction forms gases. Thus if TMB is observed in the product, this is a sign of secondary transalkylation reactions. Presence of gases is a strong sign for the dealkylation reaction.

Detailed mechanism of toluene disproportionation over ZSM-5 zeolite was reported by Xiong et al. [1]. Two different reaction pathways were proposed: methyl transfer mechanism (formation of a methoxy group on the zeolite surface) and the diphenyl methane mechanism. It was shown that toluene disproportionation does not require Brönsted acid sites of a high acid strength (present in H-ZSM-5 zeolite) to proceed, and the rate of the reaction is controlled by the concentration of acid sites, which is higher in zeolite Y compared to H-ZSM-5 [1]. Meshram [16] identified two types of active sites in H-ZSM-5; one promoting disproportionation and the other dealkylation of toluene. The latter sites were found to be suppressed by modifiers incorporation.

In 2002, a study on toluene disproportionation over modified ZSM-5 zeolite catalyst was conducted by Kareem et al., [6]. In this study, toluene disproportionation to produce benzene and *p*-xylene has been carried out using ion-exchanged HZSM-5 catalyst in a down-flow continuous fixed-bed reactor. The results indicate an increased toluene

conversion, as well as higher percentage of *p*- xylene yield beyond the equilibrium predicted level on Ni exchanged catalyst. On the other hand, Mg and Cr exchanged catalysts give the lowest yields.

Regarding the kinetic of toluene reaction, it is still debated whether this reaction follows first or second order kinetics. Aniek et al [17] reported a first order for toluene reaction over Cu/AlF3-Y zeolite. Beltrame et al [18] reported a second order reaction between two adsorbed toluene molecules over ZSM-5. A first order kinetic was proposed however, by Nayak and Riekert [19] and Bhaskar and Do [20]. Dooley et al [21] used Y-zeolite containing Ni for toluene disproportionation. Most of their reactions were adequately fitted by second order kinetics. Hydrogen was used as carrier gas in most of these papers and low coke formation, hence, no deactivation effect was considered in their modeling. Uguina et al [15] carried out the reaction over ZSM-5 zeolite in the absence of hydrogen. Das et al [22] carried out a kinetic study for toluene disproportionation over modified MFI aluminosilicate using hydrogen as a carrier gas. Their data was best fit with an irreversible first order kinetics. Their model does not consider catalyst deactivation. They attributed this to the feature of ZSM-5 zeolite which does not allow coke formation and deposition especially inside the channels of MFI. A reversible heterogeneous model was used to represent toluene disproportionation. Autor and Hofman [12] reported that the kinetics of toluene disproportionation catalyzed by the optimal Cr-pillared clay can be described by a pseudo-first order expression. Recently, Tsai et al [23] derived reversible second order kinetics for toluene disproportionation over mordenite zeolite.

It is obvious that most of the previous studies have used hydrogen as a carrier gas and have assumed low coke formation (in presence or absence of hydrogen). Hence, no deactivation factor was considered in toluene reactions. In a previous study, [24] the effect of Y-zeolite acidity on m-xylene conversion has been investigated. It was found; however, Y-zeolite affected only the reaction selectivity and it did not alter much the catalyst activity. In the present study, it is the objective of the study to highlight the role of Y-zeolite acidity on toluene transformation. The Y-zeolites have been steamed at different conditions to change the acidity and no metal was added to them. The reaction is carried out over a fluidized bed reactor over Y-zeolite catalyst and with no hydrogen at atmospheric pressure. The reaction takes place in a relatively short contact time (3 sec -15 sec) at different temperatures. During toluene reaction, an appreciable coke is deposited (Up to 1.7 wt % coke was formed) over the surface of the catalyst which leads to partial catalyst

deactivation. Two pseudo homogenous models were used to fit toluene transformation. These models include two different deactivation functions to account for coke deposition effect on the intrinsic catalyst activity.

2. Experimental Procedure

2.1 The Riser Simulator

All the experimental runs were carried out in the Riser Simulator. This reactor is a novel bench scale equipment with internal recycle unit invented by de Lasa [25] to overcome the technical problems of the standard micro-activity test (MAT), and it is fast becoming a valuable experimental tool for reaction evaluation involving model compounds [26,27], and also for testing and developing new FCC in VGO cracking [28]. The Riser Simulator consists of two outer shells, the lower section and the upper section which allow to load or to unload the catalyst easily. The reactor was designed in such way that an annular space is created between the outer portion of the basket and the inner part of the reactor shell. A metallic gasket seals the two chambers with an impeller located in the upper section. A packing gland assembly and a cooling jacket surrounding the shaft provide support for the impeller. Upon rotation of the shaft, gas is forced outward from the center of the impeller towards the walls. This creates a lower pressure in the centre region of the impeller thus inducing flow of gas upward through the catalyst chamber from the bottom of the reactor annular region where the pressure is slightly higher. The impeller provides a fluidized bed of catalyst particles as well as intense gas mixing inside the reactor. A detailed description of various Riser Simulator components, sequence of injection and sampling can be found in Kraemer [28]. A schematic diagram of the Riser Simulator is given in Fig 1.

2.2 Materials

Y zeolite was obtained from Tosoh Company. The Na-zeolite was ion exchanged with NH_4NO_3 to replace the sodium cation with NH_4^+. Following this, NH_3 was removed and the H form of the zeolite was spray-dried using kaolin as the filler and silica sol as the binder. The resulting 60-μm catalyst particles had the following composition: 30 wt% zeolite, 50 wt% kaolin, and 20 wt% silica sol. The process of sodium removal was repeated for the pelletized catalyst. Following this the catalyst was calcined for a period of 2 hr at 600^{o}C. Following this, the catalyst was calcined at 600^{o}C for 2 h. Finally, the fluidizable catalyst particles (60 μm average size) were treated with 100% steam at different temperatures and time to obtain the dealuminated Y (designated USY) zeolites. The

steaming conditions and the catalyst main properties are reported in Table 1. Surface area was measured using the BET method.

Analytical grade (99% purity) pure toluene was obtained from Sigma-Aldrich. All chemicals were used as received as no attempt was made to further purify the samples.

2.3 Procedure

Regarding the experimental procedure in the Riser Simulator, 0.8g of catalyst was weighed and loaded into the Riser Simulator basket. The system was then sealed and tested for any pressure leaks by monitoring the pressure changes in the system. Furthermore, the reactor was heated to the desired reaction temperature. The vacuum box was also heated to around 250^{o}C and evacuated at around 0.5psi to prevent any condensation of hydrocarbons inside the box. The heating of the Riser Simulator was conducted under continuous flow of inert gases (argon) and the process usually takes few hours until thermal equilibrium is finally attained. Meanwhile, before the initial experimental run, the catalyst was activated for 15 minutes at 620^{o}C in a stream of argon. The temperature controller was set to the desired reaction temperature, in the same manner the timer was adjusted to the desired reaction time. At this point the GC is started and set to the desired conditions.

Once the reactor and the gas chromatograph have reached the desired operating conditions, the feed stock was injected directly into the reactor via a loaded syringe. After the reaction, the four port valve immediately opens ensuring that the reaction was terminated and the entire product stream sent on-line to the analytical equipment via a pre-heated vacuum box chamber.

2.4 Analysis

The riser simulator operates in conjunction with a series of sampling valves that allow, following a predetermined sequence, one to inject reactants and withdraw products in short periods of time. The products were analyzed in an Agilent 6890N gas chromatograph with a flame ionization detector and a capillary column INNOWAX, 60-m cross-linked methyl silicone with an internal diameter of 0.32 mm.

Coke deposited on spent catalysts is determined by a common combustion method. In this method, a carbon analyzer multi EA 2000 (Analytikjena) is used. Oxygen is supplied to the unit directly. A small amount of the spent catalyst (0.35 g) is used for the analysis. The coke laid out on the sample during reaction experiments is burned completely

converting the carbonaceous deposit into carbon dioxide. The amount of coke formed is determined by measuring the moles of carbon dioxide.

3. Results and Discussions

Catalytic experiments were performed in a riser simulator using different catalysts. Experiments were carried out at catalyst/toluene ratio of 5 (weight of catalyst = 0.81g, weight of reactant injected = 0.162g); residence times of 3, 5, 7, 10, 13 and 15 s; and temperatures of 400, 450 and 500^{o}C. During the course of the investigation, a number of runs were repeated to check for reproducibility in the conversion results, which was found to be excellent. Typical errors were in the range of ± 2%.

3.1 Catalyst Characterization

The BET surface area was measured according to the standard procedure ASTM D-3663 using Sorptomatic 1800 Carlo Erba Strumentazione unit, Italy. The acid property of the catalyst was characterized by NH_3 temperature-programmed desorption (NH_3-TPD). In all the experiments, 50 mg of sample was outgassed at 400^{o}C for 30 min in flowing He and then cooled down to 150^{o}C. At that temperature, NH_3 was adsorbed on the sample by injecting pulses of 2 µl/pulse. The injection was repeated until the amount of NH_3 detected was the same for the last two injections. After the adsorption of NH_3 was saturated, the sample was flushed at 150^{o}C for 1 h with He to remove excess NH_3, and then the temperature was programmed at 30 ^{o}C/min up to 1000^{o}C in flowing He at 30 ml/min. Flame ionization detector was used to monitor the desorbed NH_3. The results of the catalyst characterization are presented in Table 1.

3.2 Conversion of Toluene

A steamed sample of the used catalyst (USY-1) with 0.033 mmole/g total acidity and 155 m^2/g surface area was used. As shown in Table 2, using this catalyst, no appreciable transformation of toluene was found**.** Consequently, non-steamed catalyst (H-Y) with higher acidity was used in this study. Mildly steamed catalysts (USY-2 and USY-3) were also used for comparison purpose (section 3.3).

Using the current catalyst (H-Y) with high acidity has increased toluene reactivity and a better conversion was obtained than that of USY-1 catalyst with lower acidity. Table 3 shows that toluene conversion increases with both contact time and reaction temperature. However, the temperature role on toluene conversion was found to be mild above 450^{o}C.

The product distribution on the other hand was extremely affected by temperature as shown in Table 3. Meshram and Chem [16] reported similar effect of temperature on toluene conversion using ZSM-5 zeolites. It was found that the conversion was not sensitive to temperature change above 500^{0}C. However, benzene was constantly increasing with temperature.

Toluene transformation produces mainly benzene and xylene isomers (equilibrium distribution) and small amount of gases and TMB at low temperature (350^{0}C). This result suggests that at low temperature, toluene mainly transforms through disproportionation and the secondary reactions (xylene transalkylation and xylene dealkylation) are not significant. Since benzene is produced by both primary and secondary reactions, it is not surprising to see benzene yield increasing at all reaction times and temperatures (Fig 2).

Fig 3 shows xylenes yield as a function of both conversion and temperature. It is clear that the slope is highest at 350 ^{o}C and then starts decreasing with temperature reaching a minimum at 550 ^{o}C. This behavior suggests the consumption of xylenes by dealkylation at higher temperatures. Similar result was found by Cejka et al [29] with trimethylbenzene reaction, when tetra-methylbenzene (disproportionation product) was found decreasing with temperature. Table 3 reveals the low yield of TMB which rules out any significant consumption of xylenes via disproportionation. This result is in agreement with Uguina et al [15].

As shown in Fig 4, it is clear that gas yields rise with both contact time and reaction temperature. Temperature effect on gas yield was considerable. For example, at 20 % conversion, the gas yield is 0.5 wt% and 3.7 wt% at 350 ^{o}C and 550 ^{o}C respectively. Thus, increasing reaction temperature from 350 ^{o}C to 550 ^{o}C has increased gas yield by seven fold. Furthermore, at these temperatures xylenes yield, as shown in Fig 3, is 7.7 wt% and 5 wt% at 350 ^{o}C 550 ^{o}C respectively. It can be seen that xylenes yield decreases with temperature, while gas yield increases. Fig 5 shows that at constant toluene conversion (18 %), the influence of reaction temperature on gases yield is opposite to that on xylenes yields. This suggests that as temperature increases the secondary xylenes dealkylation reaction rate also increases producing more gases. Analyzing gas content, it was found that it includes mainly paraffin gases; about 60 wt % propane and 35 wt % butane. Since no appreciable amount of C1 and C2 gases are found in the product, it can be said that no significant monomolecular dealkylation for either toluene or xylene takes place under our reaction conditions. Thus it seems that the formation of these gases proceeds via paring reaction [24,29]. Since TMB

yield is not significant at our reactions condition, this would strengthen the suggestion that xylenes dealkylation is a very important reaction and its rate increases drastically with temperature.

As temperature increases, a change in product distribution is noticed. Benzene / Xylene ratio (B/X) increases proportionally with temperature as shown in Fig 6. Similar trend for B/X with temperature was observed by several researchers [16, 20, 22]. It is depicted in Fig 6 that, B/X ratio is maximum at low toluene conversion and decreases as conversion increases. This result suggests that toluene dealkylation might be a primary reaction producing benzene and gas which explains the initial high B/X. Bhaskar and Do [20] have observed similar behavior for B/X at low conversion. They attributed this trend to the high dealkylation rate of xylenes at low toluene conversion. However, as conversion increases, xylenes concentrations also increase and xylenes dealkylation becomes more prominent [15]. Thus two dealkylation reactions might take place, a primary toluene dealkylation and a secondary xylenes dealkylation. Both dealkylation reactions have crucial role on B/X ratio. At much higher temperature (550^{o}C), B/X seems to be constant and not a function of conversion. It is relevant to mention that most researchers [16,20,22] have reported B/X greater than unity.

Coke was also measured at different conditions. Table 4 reveals the amount of coke deposition. It is clear that this amount varies with reaction condition. However, the ratio of coke wt % /(toluene conversion) is almost constant and equal to 0.065 at all reaction conditions. This is the basis of Reactant Conversion decay model [30] which will be used in the present study.

3.3 Comparison between H-Y, USY-2 and USY-3 catalysts.

A comparison study was carried out using USY-2 and USY-3 with lower acidity than H-Y and higher acidity than USY-1 catalyst. Table 2 shows that toluene conversion increases with acidity. The catalyst activity is in the following order H-Y>USY-3>USY-2>USY-1. Furthermore, Y-zeolite acidity has to be higher than 0.05 mmol/g in order to get an appreciable toluene conversion. However, toluene conversion does not necessarily mean disproportionation. Fig 7 shows comparison between xylene yields which can be used as an indicator for disproportionation reaction for these catalysts at the same conditions. It can be seen from this figure that although toluene conversion increases with acidity,

disproportionation reaction decreases. Thus, it can be concluded that Y-zeolite acidity controls toluene conversion as well as reaction selectivity. In order to have an appreciable toluene conversion in the present experimental conditions, acidity has to increase from 0.033 to 0.1 mmol/g. It is important to note that our experimental conditions involve no hydrogen and our catalysts were not impregnated by any metal.

3.4 Kinetic modeling

The disappearance of toluene in the riser simulator (batch reactor) can be represented by the following equation;

$$\frac{-V}{W_c}\frac{dy_A}{dt} = k'_0 \exp\left[\frac{-E_R}{R}\left(\frac{1}{T}-\frac{1}{T_0}\right)\right]\varphi\, y_A \qquad (1)$$

where, T_0 is the average temperature used during the reaction experiments and y_A and E_R are toluene mass fraction and activation energy reactively. The reactor volume is V and Wc is the mass of catalyst. φ is the intrinsic decay function. Several models have been used to account for catalyst decay. One of the most famous is time on stream model.

3.4.1 Time on stream model (TOS)

One classical approach while describing catalyst decay is to consider catalyst decay as a function of time-on-stream. A classical relationship is the one proposed by Voorhies [31];

$$\varphi = \exp(-\alpha t) \qquad (2)$$

where α is a constant and t is the time the catalyst is exposed to a reactant atmosphere (time –on-stream).

By substituting eq.2 into eq.1 and integrating the resulting equation, the following is obtained;

$$y_A = \exp\left[-\frac{W_c k'_0 \exp\left(-\frac{E_R}{R}\left[\frac{1}{T}-\frac{1}{T_0}\right]\right)}{V\alpha}(1-\exp(-\alpha t))\right] \qquad (3)$$

Once the decay model based on the time-on-stream, in the context of the Riser Simulator was established (eq.3), it was tested under a number of operating conditions as follows; a) six different reaction times (3, 5, 7, 10,13 and15 seconds), b) four different temperatures (350, 400, 450, and 500^{o}C), c) a single catalyst/feed ratio (catalyst/feed = 5).

The three model parameters k_0', E_R, and α were determined using non-linear regression (MATLAB package). Table 5 reports the parameters obtained and the limited spans for the 95% confidence interval. Fig 8 shows the comparison of the experimental and model predicted conversions (eq.3). In addition, Fig 9 reports the random distribution of residuals between experiments and modeling conversions.

3.4.2 Reactant conversion model (RC)

It was demonstrated by Al-Khattaf and de Lasa [30] that a catalyst activity decay function can be conveniently expressed as a function of converted reactant. This decay model relates catalyst deactivation to the extent of conversion and have been successfully tested for modeling 1,2,4-tri-methyl-benzene [32], xylenes reactions [27], cracking of cumene [30], and 1,3,5-tri-iso-propylbenzene [33].

This model was developed based on following equation;

$$\frac{dX_C}{dy_A} = A \qquad (4)$$

where A lumps a group of constant parameters and X_c is the coke mass fraction based on the catalyst weight.

By integrating eq.4 between 0 and X_C and between 1 and y_A, the following equation is obtained;

$$X_C = A(1 - y_A) \qquad (5)$$

with $$A = -\frac{\nu_c W_{hc} MW_c}{W_c MW_A} \qquad (6)$$

Once this first step of relating the conversion of reactant to the coke fraction is established, the following step in the analysis is to consider a catalyst activity decay function based on coke concentration as proposed by Froment and Bischoff [34];

$$\varphi = \exp(-\delta X_C) \qquad (7)$$

However, given the relationship between the coke concentration on catalyst, X_c and the weight fraction of toluene, y_A as given by eq.5 the following equation is obtained;

$$\varphi = \exp(-\lambda(1 - y_A)) \qquad (8)$$

where $$\lambda = A\delta \qquad (9)$$

The obtained result can be substituted in eq.1 and the following equation, describing the rate of reaction consumption is obtained;

$$\frac{-V}{W_c}\frac{dy_A}{dt} = k'_0 \exp\left(\frac{-E_R}{R}\left[\frac{1}{T}-\frac{1}{T_0}\right]\right)\exp(-\lambda(1-Y_A)y_A \qquad (10)$$

Thus, the catalyst activity decay model based on reactant conversion given by eq10 involves three parameters k'_0, E_A, andλ.

Following this, a non-linear regression involving eq.10 with three adjustable parameters was considered using MATLAB software. Table 6 reports the set of parameters obtained and the limited spans for the 95% confidence interval. Figs 10 and 11 report the comparison of model results.

Regarding the activity decay model, based on reactant conversion, one main assumption is given by eq 4. In fact one main consideration of the model that A is a constant parameter not affected by toluene conversion;

$$A = \frac{X_C}{(1-y_A)} \qquad (11)$$

In order to check the validity of this assumption a number of independent runs were developed and in each of them, in addition to the measurement of toluene conversion, the coke formed was determined. On this basis the $X_c/(1-y_A)$ group was calculated for each run independently. It was observed that as reported in Table 4, A is equal to 0.065±0.007 for the different temperatures and contact times used in the study. The confidence limits for A are in the ±10% mainly as a result of uncertainty on the measurement of Xc concentration on catalyst. The A parameter can be assumed constant (see Fig 12) and this validates the process of numerical integration of eq(10) adopted to calculate the E_R, k'_0, and λ parameters.

Finally and considering that the determined λ parameter was 1.5 and adopting A =0.07, then it results that δ =23.1. Thus eq.7 can be also reported as

$$\varphi = \exp(-23.1X_C) \qquad (12)$$

It can be also mentioned that X_c for toluene transformation (in the present reaction conditions) has typically a value in the range of 0.01 –0.02 mass fraction. Then at X_c =0.015, φ = 0.70 or 30% of the catalyst activity is lost at 0.15 g coke/g catalyst concentration.

In summary, the model developed as a function of toluene conversion, in the context of the present study, is shown to be adequate for predicting toluene conversion for a large

range of conversions, temperatures, and reaction times. It should be stressed that this decay model was developed for this reaction conditions free of transport constrains and in this context it can be considered an "intrinsic decay function" model that can be applied to the transformation of other hydrocarbon species on the same type of Y-zeolites.

4. Conclusions

The following conclusions can be drawn from the catalytic transformation and modeling of toluene over the present catalyst in the riser simulator under the conditions of the experimental study:

1. The conversion of toluene was found to increase with contact time and temperature. It was observed that the secondary xylenes dealkylation reaction becomes vital at high temperatures leading to the increase in B/X ratio and gases. The yield of TMB was not found significant which indicates that the secondary transalkylation reactions between two xylenes molecules or between a toluene molecule and a xylene molecule do not take place to an appreciable extent.

2. It was found that Y-zeolite acidity has complete control on toluene reactions. To have an appreciable conversion, acidity has to be greater than 0.05mmol/g. Acidity in the range of 0.1-0.2 mmol/g favors disproportionation reaction producing more xylenes. While acidity greater than 0.2 mmol/g favors dealkylation reaction producing more gases.

3. Toluene conversion reaction was modeled using two different deactivation functions. One based on time on stream deactivation and the other is based on reactant conversion. Both models have resulted in similar kinetic constants. The parameters optimized to the experimental data gave a good prediction of the overall reaction kinetics for toluene transformation in our experimental conditions. Thus, providing significant evidence that the 'reactant converted' decay model can be adequately utilized to account for the catalyst deactivation in similar reaction systems.

Acknowledgement

This project is supported by the King AbdulAziz City for Science & Technology (KCAST) under project # AR-22-14. Also the support of King Fahd University of Petroleum & Minerals is highly appreciated.

Nomenclature

C_i concentration of specie *i* in the riser simulator (mole/m^3)

CFL confidence limit

E_i apparent activation energy of *i*th reaction, kJ/mol

k apparent kinetic rate constant (m^3/kgcat.sec).

$$= k'_0 exp[\frac{-E_R}{R}(\frac{1}{T} - \frac{1}{T_0})$$

k'_o Pre-exponential factor in Arrhenius equation defined at an average temperature [m^3/kgcat.sec], units based on first order reaction

MW_i molecular weight of specie *i*

r correlation coefficient

R universal gas constant, kJ/kmol K

t reaction time (sec).

T reaction temperature, K

To average temperature of the experiment, 698 K

V volume of the riser (45 cm^3)

W_c mass of the catalysts (0.81 gcat)

W_{hc} total mass of hydrocarbons injected in the riser (0.162 g)

y_i mass fraction of *i*th component (wt%)

Greek letters

α apparent deactivation constant, s^{-1} (TOS Model)

φ apparent deactivation function, dimensionless

Literature Cited

1. Xiong, Y., Rodewald, P. G., and Chang, C. D. *J. Am. Chem. Soc*. **1995**, 117, 9427.

2. Kim, J. H., Namba, S., and Yashima T. *Appl. Catal*. A **1992**, 83, 51.

3. Cejka, J and Wichterlova, Catal. Rev; 2002, 44, 3, 375.

4. Chen, N. Y., Kaeding, W. W., and Dwyer, F. G. *J. Am. Chem. Soc.* **1979**, 101, 6783.

5. Kaeding, W.W; Che, C; Young, L.B; Weinstein, B; and Butter, S.A., *J.Catal*, **1981**, 69, 392.

6. Kareem, M. A. A., Chand, S., and Mishra, I. M. *J. of the Inst. of Engineers (India), Chemical Engineering Division*, **2002**, 83, 6-8.

7. Tsai, T.C, Liu, S.B, Wang, I, *Appl. Catal. A: Gen*., **1999**, 181 355.

8. Filho, J.G, Schmal, M. and Monteiro, J.L. *Catalysis Today,1989, 5, 4, 503.*

9. Peng, W, Komatsu, T and Yashima, T. *Microporous and Mesoporous Materials, 1998, 22, 1-3, 343.*

10. Kunieda, T, Kim, J and Niwa, M; *Journal of Catalysis, 1999, 188, 2, 431.*

11. Zheng, S, Jentys, A and Lercher, J; *Journal of Catalysis, 2003, 219, 2, 310.*

12. Auer, H and Hofmann, H; *Applied Catalysis A: General, 1993,97, 1,23.*

13. Yang, G, Nakamura, I and Fujimoto*, K; Applied Catalysis A: General, 1995, 127, 1-2, 115.*

14. Davidova, N, Peshev, N and Shopov, D; *Journal of Catalysis, 1979; 58, 2, 198.*

15. Uguina, M.A, Sotelo, J.L, and Serrano, D.P,, *Ind. Eng. Chem. Res,***1993**,32,49.

16. Meshram , N. R, Chem. Tech. *Biotechnol*, **1987**, 37, 111-112.

17. Aniek, L.E, Gerritsen, L.A, Van den Berg, P, de Jong, W.A, *J. Catal*, **1979** ,59 ,37.

18. Beltrame, P; Betrame, P.L; Carniti,P; Zuretti, G; Leofanti, G; Moretti, E and Padovan, M., *Zeolites*, **1987**,7,418.

19. Nayak, V.S and Riekert, L., *Applied Catalysis*, **1986**, 23, 403.

20. Bhaskar, G. V and Do, D.D, *Ind. Eng. Chem. Res,* **1990**, 29,355.

21. Dooley, K.M; Brignac, S.D; and Price, G.L., *Ind. Eng. Chem. Res,***1990**, 29,789.

22. Das, J, Bhat, Y.S, and Halgeri, A, *Ind. Eng. Chem. Res, **1994**,* 33, 246-250.

23. Tsai, T., Chen, W., Lai,C., Liu, S., Wang, I., Ku, C., *Catal Today*, **2004**, 97, 297-302.

24. Al-Khattaf, S, Iliyas, A, Al-Amer, A, Inui, T; Journal of Molecular Catalysis A, 2004, 225, 117.

25. de Lasa, H. T., US Patent 5 (102) (1992) 628.

26. Iliyas, A., and Al-Khattaf, S. *Ind. Eng. Chem. Res.,* **2004**, 43, 1349.

27. Iliyas, A., and Al-Khattaf, S. *Appl. Catal. A: Gen,* **2004**, 269, 225.

28. Kraemer, D. W., Ph.D. Dissertation, University of Western Ont., London, Canada 1991.

29. Cejka, J, Katrola, J, and Krejci, A, *Applied Catalysis* A; 2004, 277, 191.

30. Al-Khattaf, S, and de Lasa, H. I. *Ind. Eng. Chem. Res.,***2001***,* 40 , 5398.

31. Voorhies, A. Jr., *Ind. Eng. Chem*., **1945**, 37, 318.

32. Atias, J. A., Tonetto, G. and de Lasa, H. *Ind. Eng. Chem. Res.* **2003**, 42, 4162-4173.

33. Al-Khattaf, S, Atias, J, Jarosch, K, and H.I de Lasa, H.I," *Chem. Eng. Sci., **2002,*** 57, 4909.

34. Froment, G. F., and Bischoff, K. B. "Chemical Reactor Analysis and Design", Second Edition, J.Wiley, (1979).

List of Tables

Table 1. Physico-chemical properties of the as-prepared H-Y and dealuminated Y zeolites

	Zeolite			
	H-Y	USY-1	USY-2	USY-3
Steaming temperature (^oC)	-	800	600	600
Steaming time (h)	-	6	5	2
Average crystal size (μm)	0.9	0.9	0.9	0.9
BET surface area (m^2/g)	190	155	172	175
Total acidity (mmol/g)	0.55	0.033	0.1	0.2

Table 2: Toluene conversions (%) at different reaction conditions.

Temp (^oC)/ time (s)	USY-1 Conversion (%)	USY-2 Conversion (%)	USY-3 Conversion (%)	H-Y Conversion
400				
5	-	3.6	5.7	9.3
10	0.35	6.0	8.0	17.1
15	0.75	8.8	13	23.3
450				
5	-	5.4	7.2	10.7
10	0.52	12.0	14.3	19.6
15	0.84	17.2	20.0	26.1
500				
5	-	5.5	6.7	11.2
10	0.89	14.6	17.6	20.25
15	1.65	22.1	24	27.1

Table 3: Product distribution (wt %) at various reaction conditions for toluene H-Y

Temp (°C)/ time (s)	Conv. (%)	Gas	Benzene	*m*-xylene	*p*-xylene	*o*-xylene	Ethyl-benzene	*1,3,5* TMB	*1,2,4* TMB	*1,2,3* TMB	Total Xylene	Total TMB
350												
3	1.6	0	0.1	0.3	0.14	0.12	0	0	0	0	0.6	0
5	4.3	0	2.6	0.8	0.4	0.4	0	0	0	0	1.6	0
7	7.6	0.1	4.3	1.5	0.7	0.6	0.07	0.1	0.15	0	2.9	0.25
10	12.63	0.2	6.8	2.6	1.2	1.1	0.17	.11	0.29	0	5.07	0.4
13	16.7	0.47	8.6	3.4	1.6	1.44	0.26	0.16	0.4	0.06	6.7	0.62
15	18.25	0.5	9.2	3.8	1.8	1.6	0.3	0.18	0.44	0.06	7.5	0.68
400											0	0
3	3.8	0.07	2.3	0.7	0.33	0.3	0	0	0.1	0	1.33	0.1
5	9.3	0.37	5.0	1.8	0.82	0.8	0.14	0.09	0.24	0	3.56	0.33
7	11.6	0.43	6.2	2.2	1.0	0.95	0.2	0.11	0.3	0.04	4.35	0.45
10	17.1	0.7	8.5	3.3	1.6	1.5	0.3	0.19	0.5	0.07	6.7	0.76
13	20.15	1.1	10.0	3.9	1.8	1.7	0.4	0.22	0.6	0.08	7.8	0.9
15	23.3	1.2	11.3	4.6	2.15	2.0	0.5	0.27	0.7	0.1	9.25	1.07
450											0	0
3	6.1	0.31	3.36	1.1	0.5	0.5	0.08	0.06	0.17	0	2.18	0.23
5	10.7	0.7	5.5	1.9	0.9	0.86	0.17	0.11	0.3	0.04	3.83	0.45
7	14.3	1.3	7.1	2.4	1.14	1.1	0.25	0.15	0.39	0.06	4.89	0.6
10	19.5	1.64	9.4	3.52	1.64	1.6	0.37	1.22	0.6	0.09	7.13	1.91
13	22	2.3	10.5	3.8	1.8	1.7	0.43	0.26	0.68	0.09	7.73	1.03
15	26.1	2.45	12.2	4.7	2.2	2.1	0.53	0.3	0.8	0.12	9.53	1.22
500											0	0
3	6.7	0.66	3.5	1.1	0.5	0.5	0.1	0.06	0.18	0	2.2	0.24
5	11.2	1.3	5.7	1.8	0.82	0.82	0.18	0.11	0.31	0.05	3.62	0.47
7	15.3	2	7.1	2.2	1.0	1.0	0.23	0.14	0.36	0.06	4.43	0.56
10	20.25	3	9.7	3.1	1.4	1.4	0.34	0.2	0.53	0.09	6.24	0.81
13	23.4	4	11.2	3.4	1.6	1.6	0.4	0.24	0.6	0.09	7	0.93
15	27.12	4.4	12.7	4.11	1.9	1.9	0.5	0.27	0.75	0.11	8.41	1.13
550											0	0
3	6.9	1.0	3.66	0.94	0.44	0.45	0.09	0.06	0.16	0	1.92	0.22
5	10.5	1.8	5.45	1.4	0.64	0.66	0.15	0.083	0.24	0	2.85	0.32
7	15.1	2.6	7.3	1.88	0.87	0.9	0.21	0.11	0.33	0.05	3.86	0.49
10	18.56	3.6	9.3	2.34	1.1	1.1	0.27	0.14	0.4	0.06	4.81	0.6
13	22.5	4.5	11.2	2.82	1.3	1.36	0.33	0.17	0.46	0.08	5.81	0.71
15	26.5	5.3	13.1	3.35	1.6	1.6	0.4	0.2	0.59	0.09	6.95	0.88

Table 4: Coke formation for toluene conversions (%) at different reaction conditions over H-Y

Temp (^{o}C)/ time (s)	Conversion (%)	Coke wt%	Coke wt%/conv
400			
5	9.3	0.57	0.06
7	11.6	0.77	0.07
10	17.1	0.93	0.06
15	23.3	1.42	0.06
450			
5	10.7	0.65	0.06
7	14.3	0.93	0.07
10	19.5	1.1	0.06
15	26.1	1.53	0.06
500			
5	11.2	0.8	0.07
7	15.3	1.1	0.07
10	20.25	1.38	0.07
15	27.12	1.67	0.06

Table 5: Kinetic constants for toluene conversion (over H-Y) based on time on stream (TOS)

k_0 (cm^3/g-cat.sec)	95% CFL	E_R (kcal/mol)	95% CFL	α (1/sec)	95% CFL	r^2
1.32	0.13	3.47	0.50	0.02	0.02	0.98

Table 6: Kinetic constants (over H-Y) based on reactant conversion (RC)

k_0 (cm^3/g-cat.sec)	95% (CFL)	E_R (kcal/mol)	95% CFL	λ	95% CFL	r^2
1.22	0.12	4.0	0.16	1.5	0.95	0.99

Figure Captions

Figure 1: Schematic Diagram of the Riser Simulator

Figure 2: Benzene yield versus toluene conversions at various temperatures.

Figure 3: Xylenes yield at various temperatures.

Figure 4: Gas yield versus toluene conversion at different temperatures.

Figure 5: Gas and xylenes yields versus reaction temperature (at constant toluene conversion of 18 wt%).

Figure 6: Molar ratio of Benzene to Xylenes (B/X) at different temperatures.

Figure 7: Comparison between xylene yields for different catalysts.

Figure 8: Modeling Toluene conversion over H-Y. Decay function based on time on stream (TOS)

Figure 9: Overall comparison between the experimental results and model predictions (TOS): (♦) 350 ^{O}C; (■) 400 ^{O}C; (▲) 450 ^{O}C; (x) 500 ^{O}C;

Figure 10: Modeling Toluene conversion over H-Y. Decay function based on reactant converted model (RC)

Figure 11: Overall comparison between the experimental results and model predictions (RC): (♦) 350 ^{O}C; (■) 400 ^{O}C; (▲) 450 ^{O}C; (x) 500 ^{O}C;

Figure 12: Coke yield/(toluene conversion) vs. toluene conversion.

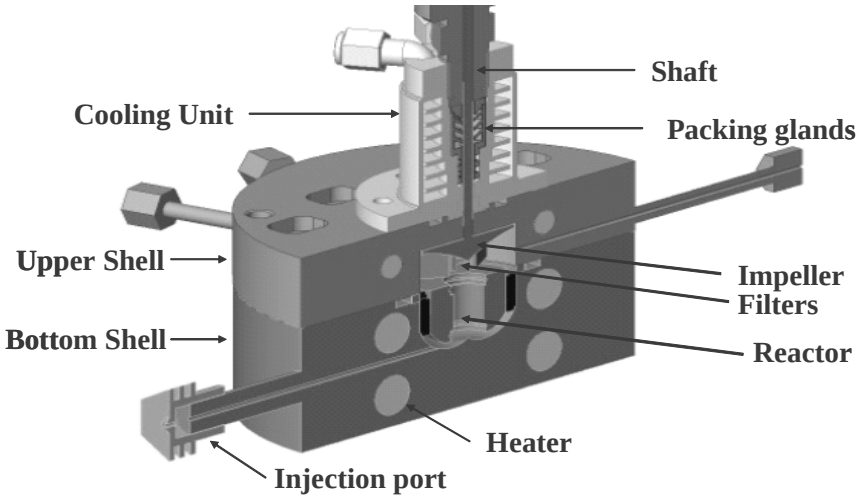

Figure 1: Schematic Diagram of the Riser Simulator

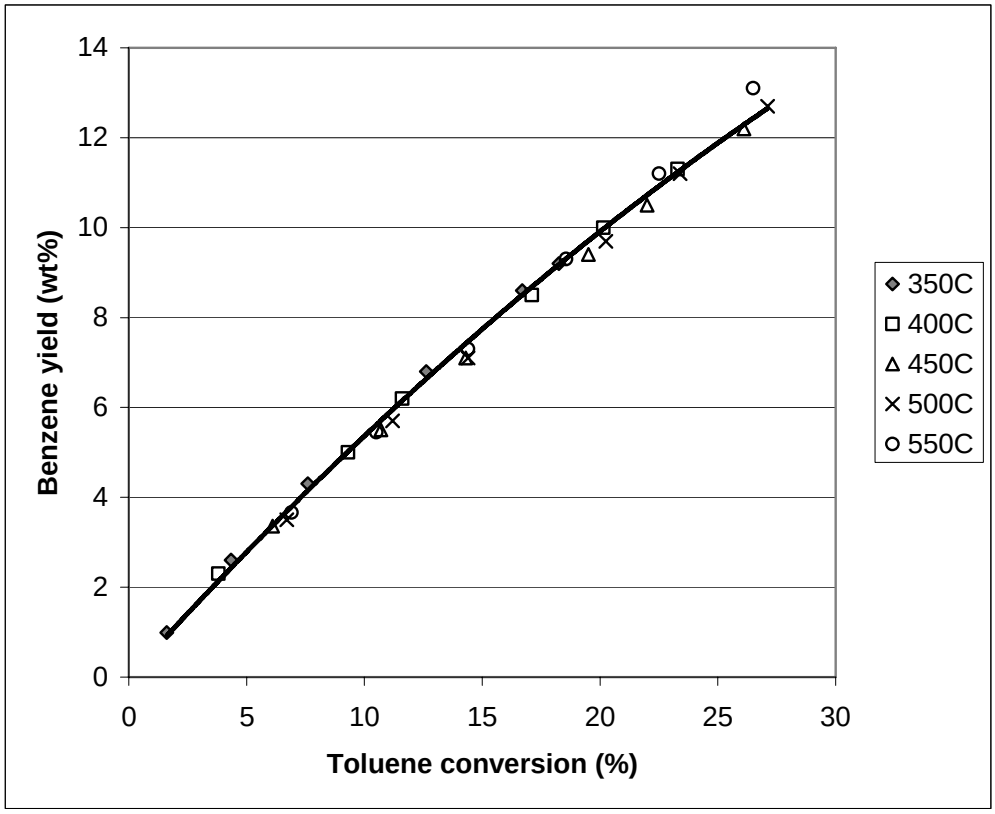

Figure 2: Benzene yield versus toluene conversions at various temperatures.

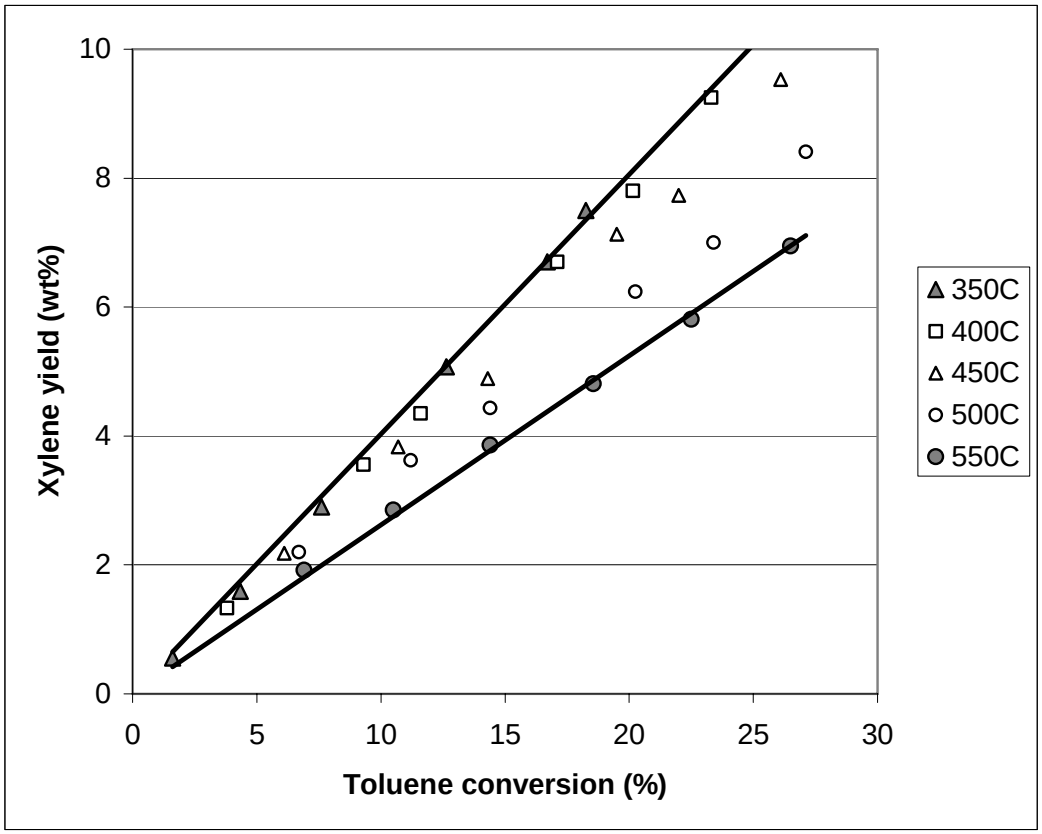

Figure 3: Xylenes yield at various temperatures.

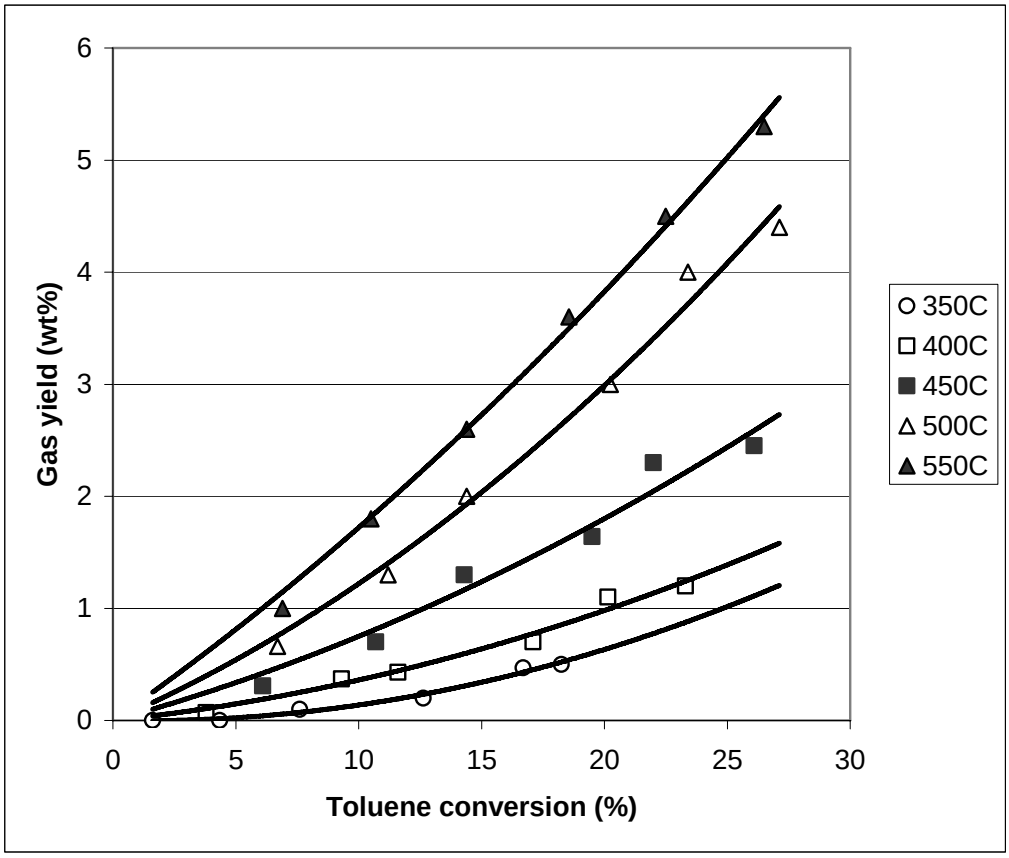

Figure 4: Gas yield versus toluene conversion at different temperatures.

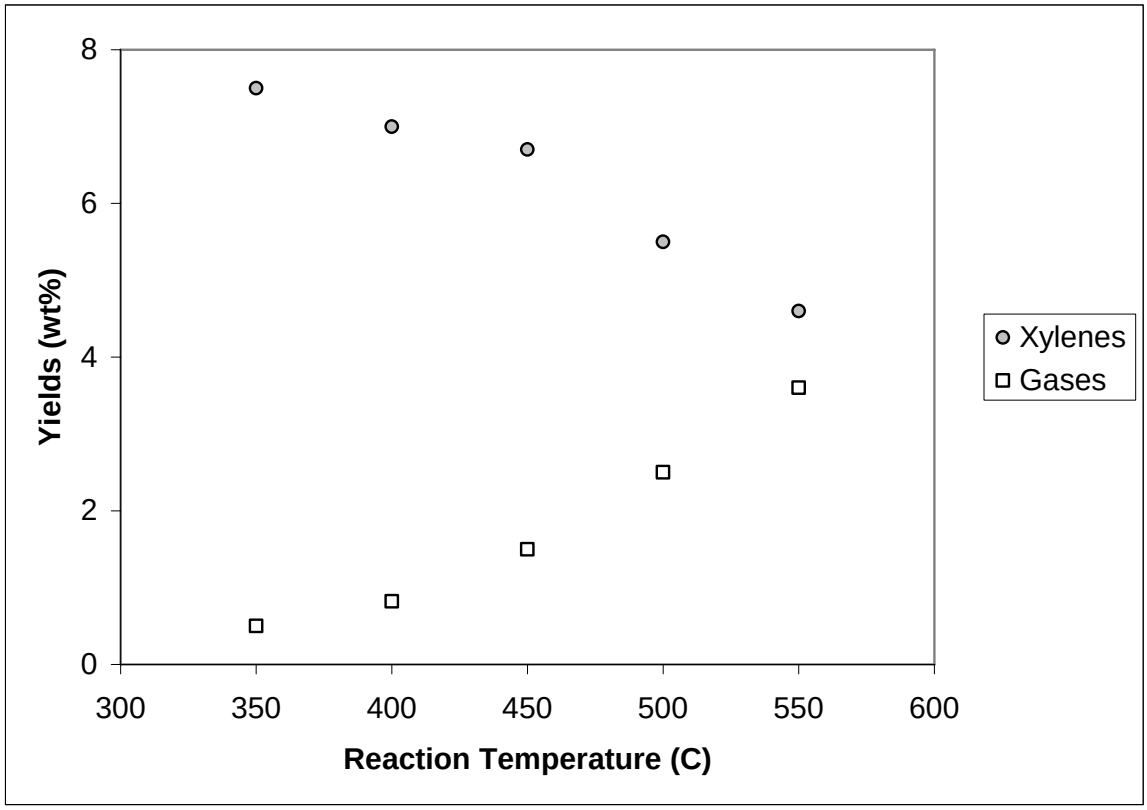

Figure 5: Gases and xylenes yields versus reaction temperature (at constant toluene conversion of 18 wt%).

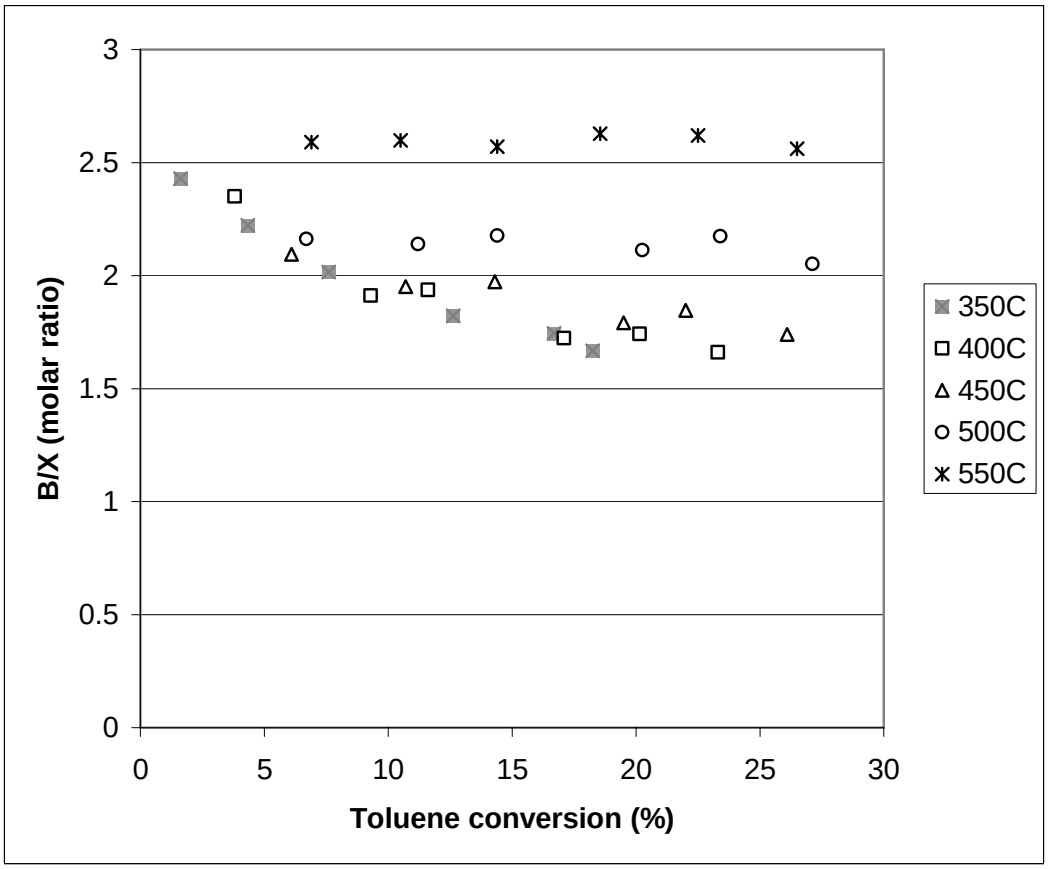

Figure 6: Molar ratio of Benzene to Xylenes (B/X) at different temperatures.

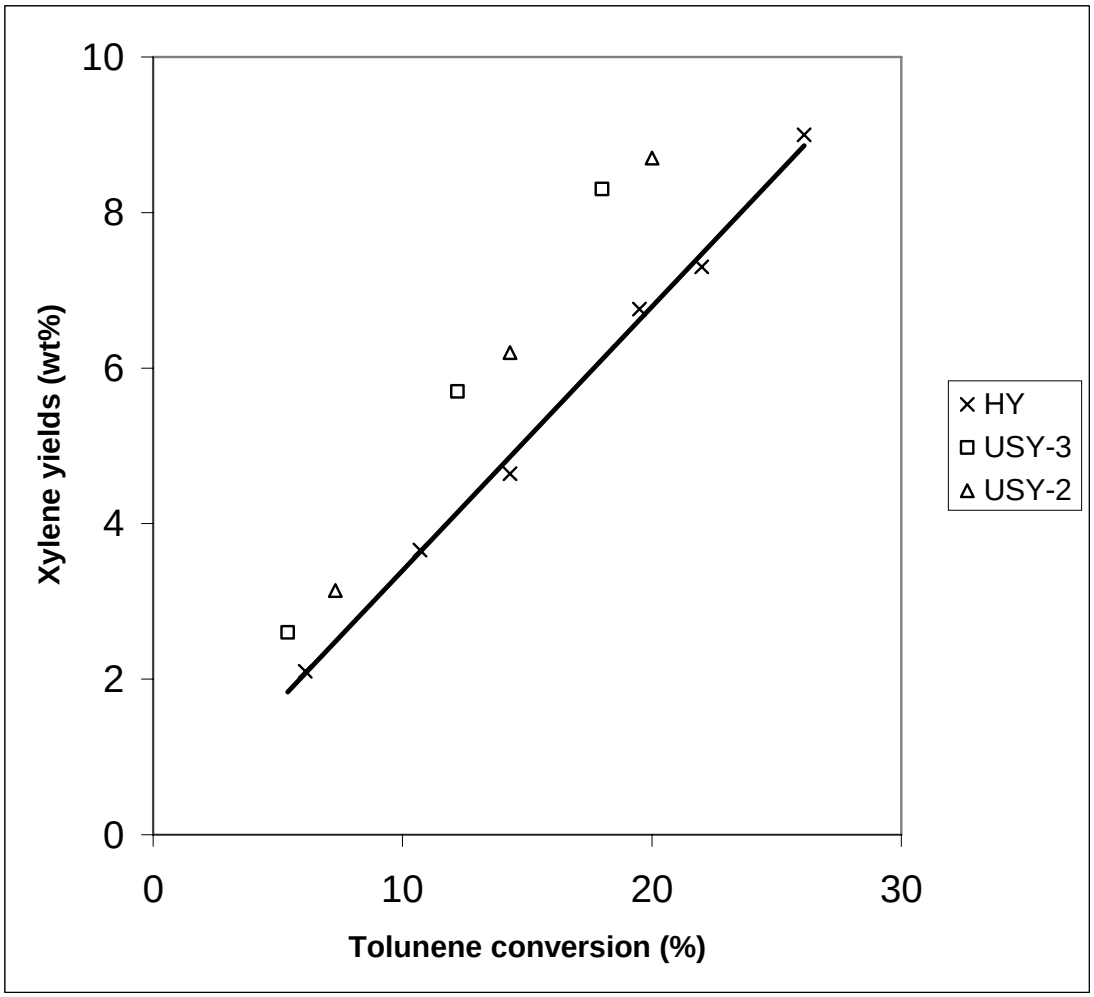

Fig 7. Comparison between xylene yields for different catalysts.

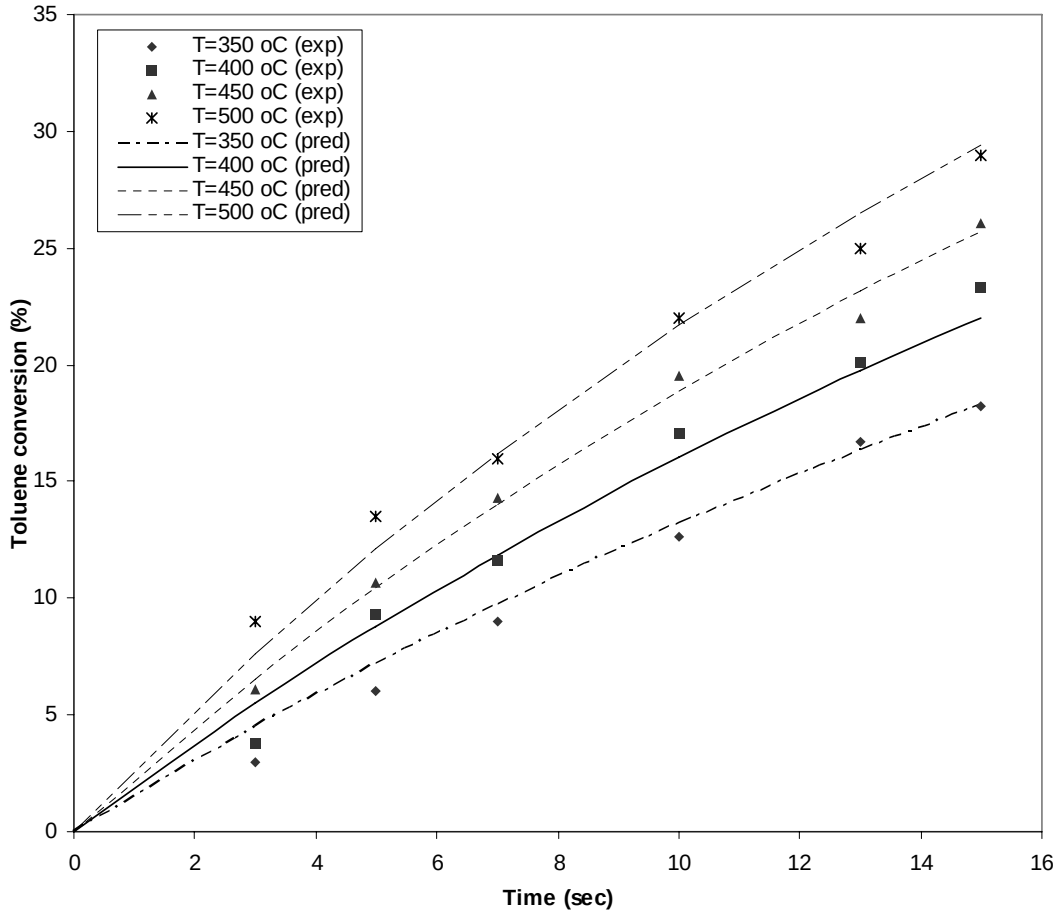

Figure 8: Modeling Toluene conversion over H-Y. Decay function based on time on stream (TOS)

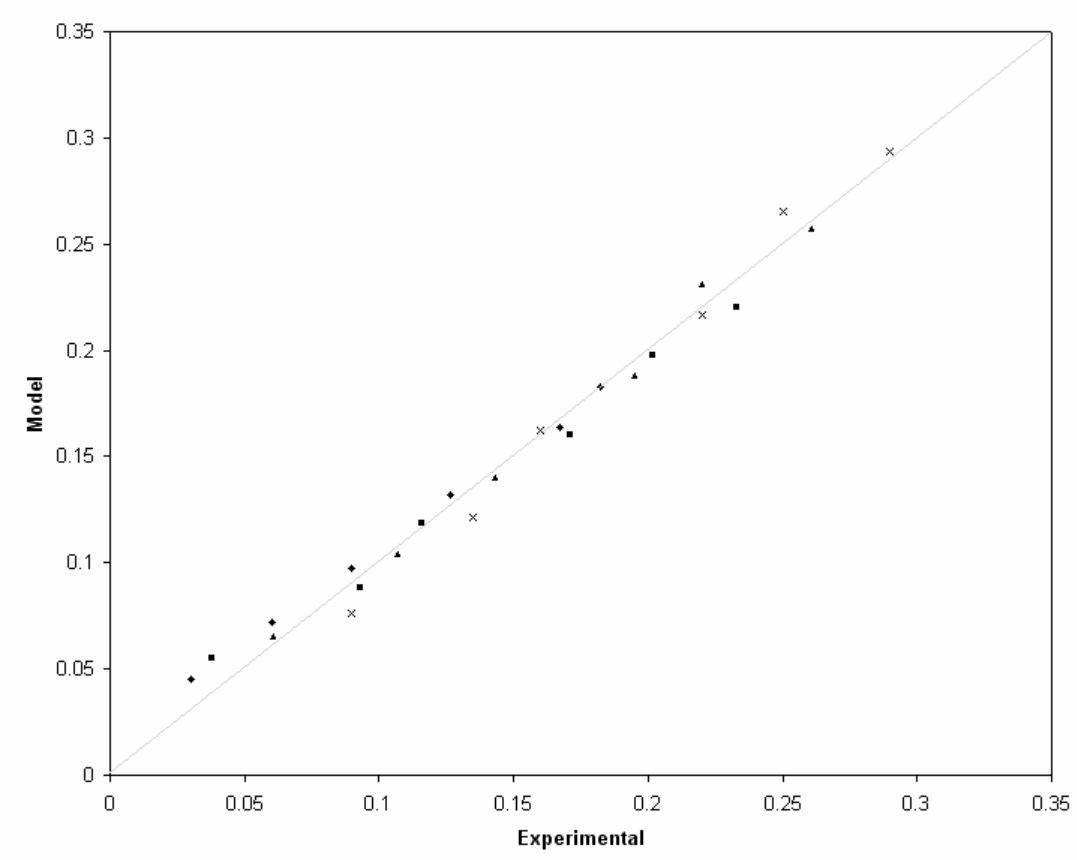

Figure 9: Overall comparison between the experimental results and model predictions (TOS): (♦) 350 ^{O}C; (■) 400 ^{O}C; (▲) 450 ^{O}C; (x) 500 ^{O}C;

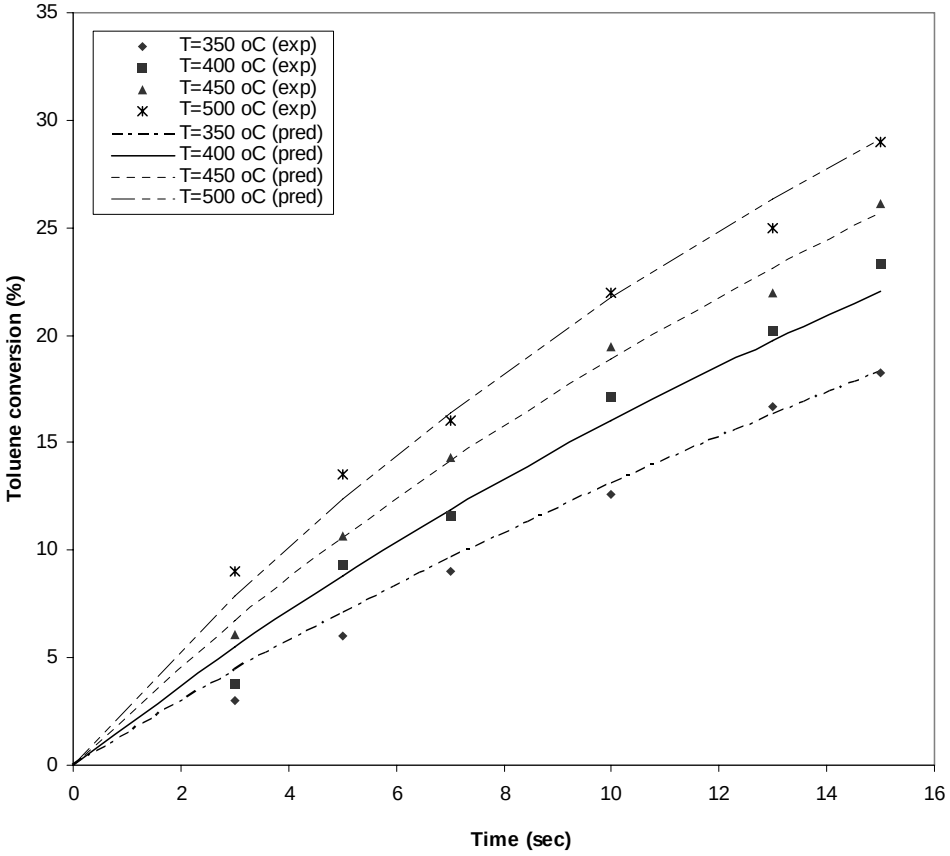

Figure 10: Modeling Toluene conversion over H-Y. Decay function based on reactant converted model (RC)

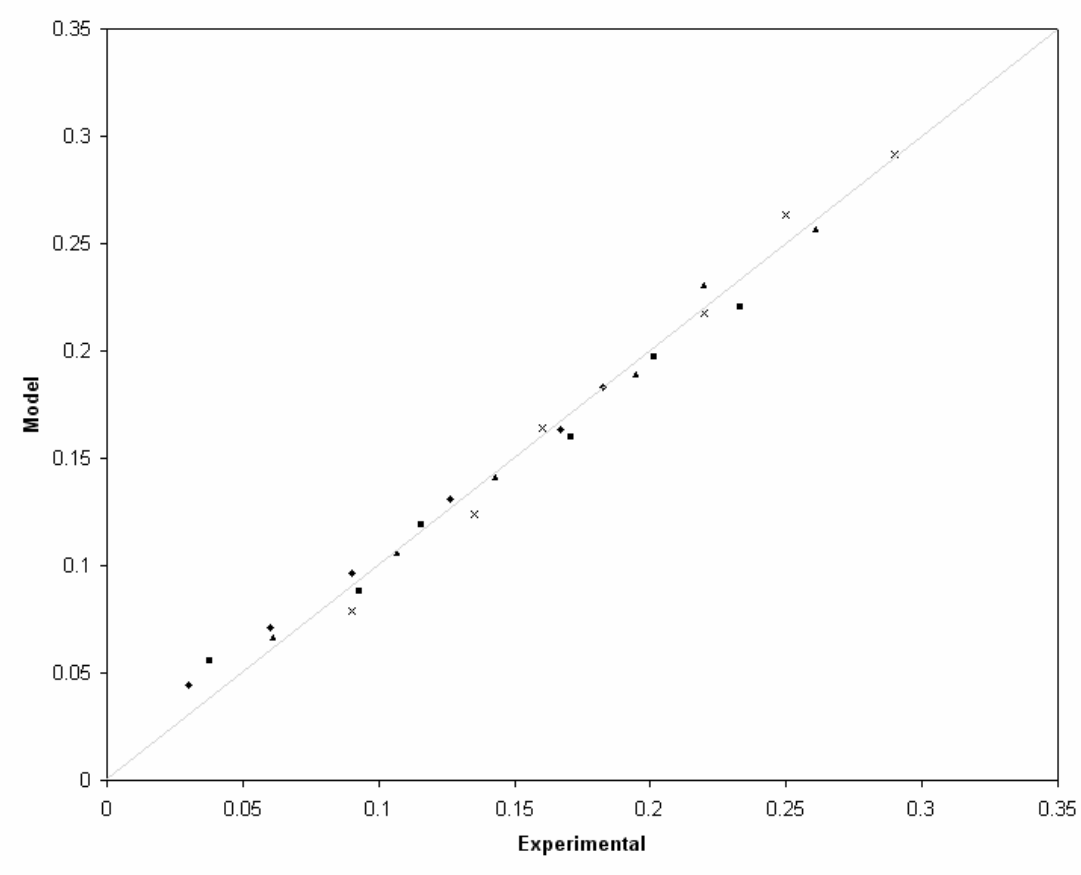

Figure 11: Overall comparison between the experimental results and model predictions (RC): (♦) 350 ^{O}C; (■) 400 OC; (▲) 450 ^{O}C; (x) 500 ^{O}C;

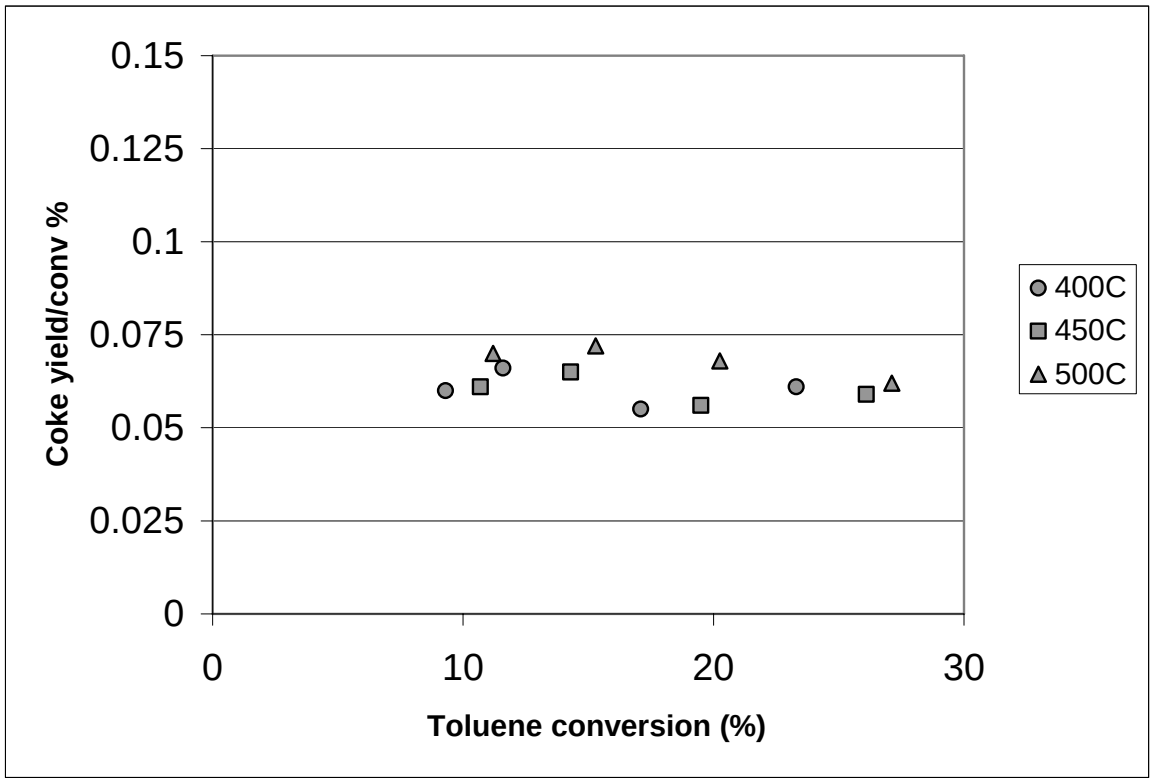

Figure 12: Coke yield/ (toluene conversion) vs. toluene conversion.